

# Electronic structure of chiral graphene tubules

R. Saito, M. Fujita, G. Dresselhaus, and M. S Dresselhaus  
*Massachusetts Institute of Technology, Cambridge, Massachusetts 02139*

(Received 27 January 1992; accepted for publication 4 March 1992)

The electronic structure for graphene monolayer tubules is predicted as a function of the diameter and helicity of the constituent graphene tubules. The calculated results show that approximately 1/3 of these tubules are a one-dimensional metal which is stable against a Peierls distortion, and the other 2/3 are one-dimensional semiconductors. The implications of these results are discussed.

It has recently been postulated<sup>1</sup> and observed<sup>2,3</sup> that graphene tubules can be formed from a single layer of graphite. Such tubules would be expected to have unique properties.

If we consider the interrelation between the two most stable fullerenes,  $C_{70}$  and  $C_{60}$ , we see that by adding one row of five armchair hexagons to  $C_{60}$  along the equator normal to a fivefold axis, we get  $C_{70}$ . This suggests adding instead  $j$  such rows of armchair hexagons<sup>1</sup> to obtain a  $C_{60+10j}$  molecule which would be in the form of a monolayer graphene tubule (armchair fiber). Similarly, by cutting the  $C_{60}$  molecule in half, normal to a threefold axis along the zigzag edges, a perfect fit can be made to a one-atom-thick cylindrical sheath consisting of  $j$  rows of nine zigzag hexagons (zigzag fiber).<sup>4</sup> This concept of graphene tubules can be extended to include chiral fibers<sup>2,5,6</sup> whose diameter and helicity are defined generally in this letter. The corresponding nucleating and terminating caps for any chiral fiber can be theoretically predicted.<sup>7</sup> Some of the general caps are hemispheres with icosahedral symmetry and other caps do not have an axis of rotation along the fiber axis. In Fig. 1, we show an example of a chiral fiber with an icosahedral cap, corresponding to a hemisphere of icosahedral  $C_{140}$ ,<sup>8</sup> the smallest diameter fullerene with group  $I$  symmetry.

Such graphene tubules are of scientific interest as a carbon fiber approaching the smallest possible outer diameter ( $\sim 10 \text{ \AA}$ ). Carbon fibers are today commercially important for their extraordinary high modulus and strength. Having made a new form of carbon suggests making a new type of carbon fiber nucleated from a hemisphere of  $C_{60}$ . Study of the mechanical and electronic properties of such tubules could provide interesting theoretical limits for the behavior of carbon fibers, especially for vapor-grown carbon fibers which have a similar structural arrangement. To nucleate cylindrical growth instead of  $C_{60}$  ball growth, some defect is needed in the cap region during the early formation stage. In general, these defective caps will introduce some chirality which is propagated in the cylindrical tubule nucleated by the cap. Experimentally, most of the observed tubules exhibit chirality.<sup>2</sup>

The chirality and the fiber diameter are uniquely specified by the vector  $\mathbf{c}_h = n_1 \mathbf{a}_1 + n_2 \mathbf{a}_2 \equiv (n_1, n_2)$ , where  $n_1, n_2$  are integers and  $\mathbf{a}_1, \mathbf{a}_2$  the unit vectors of graphite, and  $\mathbf{c}_h$  connects two crystallographically equivalent sites,  $A$  and  $A'$ , as shown in Fig. 2(a). The graphene cylinder is formed by connecting together the points  $A$  and  $A'$  and the cylin-

der joint is made along the lightly dotted lines perpendicular to  $\mathbf{c}_h$ . The fiber diameter  $d$  is defined by  $d = |\mathbf{c}_h|/\pi = a \sqrt{n_1^2 + n_1 n_2 + n_2^2}/\pi$ , where  $a = 1.42 \times \sqrt{3} \text{ \AA}$  is the lattice constant. The chiral fiber thus generated has no distortion of bond angles other than that caused by the cylindrical curvature of the fiber. This generalized description of chiral fibers [Fig. 2(b)] includes a range of orientations for  $\mathbf{c}_h$  extending from the zigzag direction [ $\theta = 0^\circ$ , or  $(n_1, n_2) = (p, 0)$ ,  $p$  is an integer] to the armchair direction [ $\theta = \pm 30^\circ$ ,  $(n_1, n_2) = (2p, -p), (p, p)$ ], which form two limiting cases. The chiral angle,  $\theta = \arctan[-\sqrt{3}n_2/(2n_1 + n_2)]$ , is defined as the angle between  $\mathbf{c}_h$  and the zigzag direction, as shown in Fig. 2(a). Since there are six definable angles for a fiber because of the hexagonal local structure, we select  $|\theta| < 30^\circ$  or  $-n_1 < n_2 < n_1$  ( $n_1 > 0$ ). Since

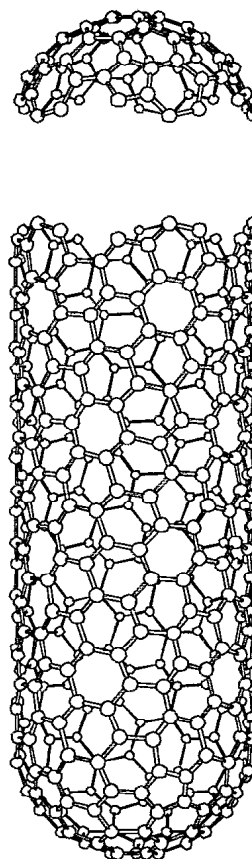


FIG. 1. A chiral fiber with hemispherical caps at both ends based on an icosahedral  $C_{140}$  fullerene. The corresponding chiral vector is  $\mathbf{c}_h = (10, 5)$ ,  $d = 10.36 \text{ \AA}$ , and  $\theta = -19.11^\circ$ .

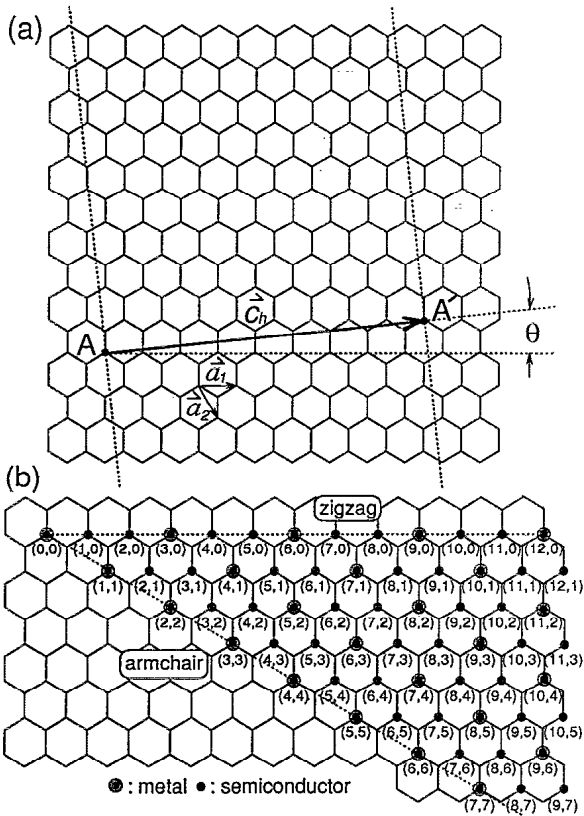


FIG. 2. (a) Graphene tubules are made by rolling a graphene sheet into a cylinder. The tubules are uniquely determined by their lattice vectors  $\mathbf{c}_h$ . The chiral angle is denoted by  $\theta$ , while  $\mathbf{a}_1$  and  $\mathbf{a}_2$  denote the unit vectors of graphite. (b) Possible vectors for chiral fibers. The circled dots and dots, respectively, denote metallic and semiconducting behavior for each fiber.

there is no mirror symmetry for a fiber, both right- ( $\theta > 0^\circ$ ) and left- ( $\theta < 0^\circ$ ) handed optical isomers are possible, as are also chiral fibers with  $|\theta| > 30^\circ$ . The chiral angle  $\theta$  should determine the optical activity of the fiber and the speed (or stability) of fiber growth.

From a theoretical standpoint, graphite tubules are interesting as the embodiment of a one-dimensional (1D) periodic structure along the fiber axis. Confinement in the radial direction is provided by the monolayer thickness of the fiber. In the circumferential direction, periodic boundary conditions apply to the enlarged unit cell that is formed in real space and the subsequent zone folding that occurs in reciprocal space. For the fiber geometry, there is some mixing of the  $\pi(2p_z)$  and  $\sigma(2s$  and  $2p_{x,y})$  carbon orbitals due to the fiber curvature, but this mixing is small and can be neglected near the Fermi level.<sup>6</sup> Thus, we consider only  $\pi$  orbitals. The two-dimensional (2D) energy dispersion relations for  $\pi$  bands of graphite,  $E_{2D}$ , are given by<sup>9</sup>

$$E_{2D} = \pm \gamma_0 \left[ 1 + 4 \cos\left(\frac{\sqrt{3}k_x a}{2}\right) \cos\left(\frac{k_y a}{2}\right) + 4 \cos^2\left(\frac{k_y a}{2}\right) \right]^{1/2}, \quad (1)$$

where  $\gamma_0$  is the nearest-neighbor overlap integral.<sup>10</sup> Eliminating  $k_x$  or  $k_y$  by using the periodic boundary condition,

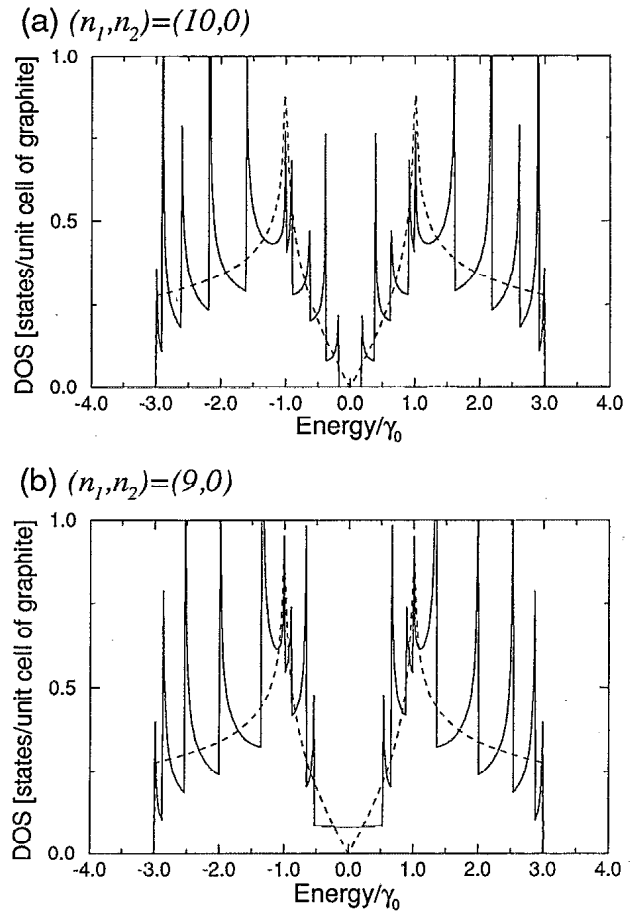


FIG. 3. Electronic density of states for two  $(n_1, n_2)$  zigzag fibers: (a)  $(10, 0)$  and (b)  $(9, 0)$ .

$$\mathbf{c}_h \cdot \mathbf{k} = 2\pi m, \quad (2)$$

where  $m$  is an integer, we get 1D energy bands for general chiral structures. In other words, 1D energy bands can be obtained by *slicing* the 2D energy dispersion relations of Eq. (1) in the directions expressed by Eq. (2).

In Figs. 3(a) and 3(b), the density of states for two zigzag fibers with  $(n_1, n_2) = (10, 0)$  and  $(9, 0)$ , respectively, are plotted in units of states per unit cell of 2D graphite. We also plot the corresponding density of states of 2D graphite (dotted lines) in both figures for comparison. The  $1/\sqrt{E}$  singularities characteristic of 1D energy bands appear at the band edges of each energy band. In Fig. 3(a), there is an energy gap at the Fermi level ( $E=0$ ), while we have a finite density of states for Fig. 3(b). Thus, we can have both semiconducting [Fig. 3(a)] and metallic [Fig. 3(b)] fibers by merely changing the fiber diameter. The energy gap for the semiconducting fibers decreases with increasing fiber diameter  $d$  and in the limit of  $d \rightarrow \infty$ , we obtain the 2D case of a zero-gap semiconductor. The condition for a fiber to be metallic is

$$2n_1 + n_2 = 3q, \quad (3)$$

where  $q$  is an integer. This condition is easily obtained by substituting the  $\mathbf{k}$  vector of the degenerate point of 2D graphite (corner of the hexagonal Brillouin zone) into Eq. (2). Since two optical isomers for  $-\theta$  and  $\theta$  give the same results for the energy gap (optical selection rules are dif-

ferent), we show chiral vectors only for  $-30^\circ < \theta < 0^\circ$  in Fig. 2(b). Here, the metallic and semiconducting fibers are denoted by circled dots and simple dots, respectively. In particular, all armchair fibers are metallic, and zigzag fibers are metallic when  $n_1$  is a multiple of three.

A finite density of states results from the crossing of two 1D energy bands at degenerate points of the 2D graphite energy-band structure. Metallic 1D energy bands are generally unstable under a Peierls distortion. However, the Peierls energy gap obtained for the metallic cases is found to be greatly suppressed by increasing the fiber diameter and the Peierls gap quickly approaches the zero-energy gap of 2D graphite.<sup>6,11</sup> Thus, if we consider finite temperatures or fluctuation effects, such a small Peierls gap can be neglected. It is surprising that the calculated electronic structure can be either metallic or semiconducting depending on the fiber diameter and on the chiral angle  $\theta$ , though there is no difference in the local chemical bonding between the carbon atoms, and no doping impurities are present.

If the distribution of  $c_h$  vectors shown in Fig. 2 is uniform, 1/3 of the fibers will be metallic and 2/3 semiconducting. However, we may obtain a larger fraction of metallic fibers if the initial seed of the fiber caps is centered about a pentagon, which yields an armchair fiber. If the initial seed is not a pentagon but a hexagon, growth of the planar graphite structure seems more likely. In this sense, nature may prefer armchair-type fibers which are metallic for all  $(p,p)$ .

From the results of this letter, one could imagine designing a minimum-size conductive wire consisting of two

concentric graphene tubules with a metallic inner tubule covered by a semiconducting (or insulating) outer tubule. These concepts could further lead to the design of mesoscopic metal-semiconductor devices with cylindrical geometry which are optically active, without introducing any doping impurities. There are, of course, many other possibilities for arranging graphene tubules with interesting potential applications which could be stimulated by the results presented here.

Two of the authors (R.S. and M.F.) have carried out this work while they are visiting scientists at MIT as Overseas Research Scholars of the Ministry of Education, Science and Culture of Japan. We gratefully acknowledge National Science Foundation Grant No. DMR88-19896 for support for this research.

<sup>1</sup>M. S. Dresselhaus, G. Dresselhaus, and R. Saito, Phys. Rev. B **45**, 6234 (1992).

<sup>2</sup>S. Iijima, Nature **354**, 56 (1991).

<sup>3</sup>M. Endo, H. Fujiwara, and E. Fukunaga, *Abstract of Second C<sub>60</sub> Symposium* (Japan Chemical Society, Tokyo, 1992), pp. 101-104.

<sup>4</sup>G. Dresselhaus, M. S. Dresselhaus, and P. C. Eklund, Phys. Rev. B **45**, 6923 (1992).

<sup>5</sup>F. Diederich and R. L. Whetten, Acc. Chem. Res. **25**, 119 (1992).

<sup>6</sup>R. Saito, M. Fujita, G. Dresselhaus, and M. S. Dresselhaus, MRS Symp. Proc. **247**, 333 (1992).

<sup>7</sup>M. Fujita, R. Saito, G. Dresselhaus, and M. S. Dresselhaus (unpublished).

<sup>8</sup>P. W. Fowler, Chem. Phys. Lett. **131**, 444 (1986).

<sup>9</sup>P. R. Wallace, Phys. Rev. **71**, 622 (1947).

<sup>10</sup>M. S. Dresselhaus and G. Dresselhaus, Adv. Phys. **30**, 139 (1981).

<sup>11</sup>J. W. Mintmire, B. I. Dunlap, and C. T. White, Phys. Rev. Lett. **68**, 631 (1992).